Electrochimica Acta 347 (2020) 136311

Contents lists available at ScienceDirect

Electrochimica Acta

journal homepage: www.elsevier.com/locate/electacta

Effect of PbS quantum dot-doped polysulfide nanofiber gel polymer electrolyte on efficiency enhancement in CdS quantum dot-sensitized TiO_2 solar cells

M.A.K.L. Dissanayake [a, *], T. Liyanage [a], T. Jaseetharan [a, b, c], G.K.R. Senadeera [a, d], B.S. Dassanayake [e]

[a] National Institute of Fundamental Studies, Hantana Road, Kandy, Sri Lanka
[b] Postgraduate Institute of Science, University of Peradeniya, Peradeniya, Sri Lanka
[c] Department of Physical Sciences, South Eastern University of Sri Lanka, Sammanthurai, Sri Lanka
[d] Department of Physics, The Open University of Sri Lanka, Nawala, Nugegoda, Sri Lanka
[e] Department of Physics University of Peradeniya, Peradeniya, Sri Lanka

ARTICLE INFO

Article history:
Received 9 March 2020
Received in revised form
19 April 2020
Accepted 22 April 2020
Available online 24 April 2020

Keywords:
Quantum dot doped electrolyte
Quantum dot sensitized solar cells
Nanofibre gel electrolyte
Efficiency enhancement
Sulfide ion conductivity

ABSTRACT

Quantum dot-sensitized solar cells (QDSSCs) are among the most promising low cost third generation solar cells. Semiconductor quantum dots have unique properties such as high molar extinction coefficients, tunable energy gap by the quantum confinement effect and the ability of multiple exciton generation. In this study, stable CdS QDSSCs were fabricated by using polysulfide liquid electrolyte and also by using cellulose acetate nanofiber-based gel electrolyte. Incorporation of PbS Q dots to the liquid or gel electrolyte showed a significant enhancement in solar cell efficiency. Under the simulated light of 100 mW cm^{-1} the efficiency of the polysulfide liquid electrolyte based CdS QD solar cells increased from 1.19% to 1.51% and the efficiency of the nanofibre gel electrolyte based CdS QD solar cells increased from 0.94% to 1.46% due to the incorporation of 5% (wt/wt) PbS Q dots into the respective electrolytes. The efficiency increase has been attributed to the increase in short circuit photocurrent density due to increased sulfide ion (S^{2-}) conductivity evidently caused by indirect ionic dissociation facilitated by PbS QDs.

1. Introduction

The ever-increasing power demand has pushed the research community to explore more efficient, environmentally friendly, and cheaper energy sources to replace the currently dominant oil and coal power plants [1,2]. Due to the low cost fabrication [3] and reasonably high theoretical efficiency, quantum dot sensitized solar cells (QDSSCs) [4] are emerging as a highly promising class of renewable energy sources. They also possess versatile properties such as high molar extinction coefficients, ability of multiple exciton generation, high stability against heat and tunable energy band gap due to the quantum confinement effect [5–9]. The best reported QDSSCs exhibit efficiency of 6–7% [10–14]. These remarkable values of the cell efficiencies have been achieved by using advanced QD systems, such as CdSe/CdTe and PbS/PbSe core shell structures etc. [15–18], and using higher light harvesting photo anodes [19–22] and the introduction of novel counter electrodes [23–26]. As for the type of basic CdS QD solar cell structures used in the present study, reported efficiencies are between 0.94% and 1.51%.

The polysulfide electrolyte, which plays a crucial role in QD regeneration and charge transfer between photo anode and the counter electrode, is a necessary component of the QDSSCs [27]. Despite the undesirable high redox potential of the (S^{2-}/S_n^{2-}) redox couple, which requires a high over potential for QD regeneration, polysulfide electrolyte has remained the most commonly used electrolyte for QDSSCs. Prevalence of the (S^{2-}/S_n^{2-}) electrolyte can be attributed to the high compatibility whereas I^-/I_3^- and Co^{2+}/Co^{3+} complexes haven not been able to achieve better photovoltaic performance with QDSSCs [28–30]. This is due to the rapid QD degradation caused by these alternative electrolytes. Hence, it is prudent to optimize the performance of the already known

* Corresponding author.
E-mail address: lakshman.di@nifs.ac.lk (M.A.K.L. Dissanayake).

https://doi.org/10.1016/j.electacta.2020.136311
0013-4686/

polysulfide electrolytes and thereby enhance the efficiencies of QDSSCs. Currently, the performance enhancement of the polysulfide electrolyte is mainly carried out by the addition of additives [31–34]. In addition to the enhancement of the photovoltaic performance recent research have also been focused on methods to increase the stability of the polysulfide electrolyte [35]. In this context, the formation of polymer based quasi solid or gel electrolytes has substantially increased the stability of the electrolyte mainly due to the semi-solid nature of the electrolyte which drastically reduces the evaporation of the electrolyte [36]. However, due to the poor ionic conductivity of these quasi-solid electrolytes, the photovoltaic performance of the solar cells is also reduced [16,18–41]. In this context, effect of doping PEO based polymer electrolytes with ZnS capped CdSe quantum dots has been reported by Singh et al. [50]. In the present study, we have focused on the development of a gel electrolyte formed by incorporating a polysulfide solution electrolyte in a cellulose nanofibre membrane while compensating for the reduction of CdS QD solar cell performance by improving the electrolyte ionic conductivity using PbS Quantum dots as an electrolyte additive.

2. Experimental

2.1. Materials

Fluorine-doped tin oxide (FTO) coated glass (8 Ω cm^{-2}, Solarnoix), Titanium dioxide P90 powder (Evonik), Hydrochloric acid (37%, Sigma-Aldrich), Titanium dioxide powder P25 (Degussa), Triton X-100 (Sigma-Aldrich), Polyethylene glycol (99.8%, Sigma-Aldrich), Methanol (99.8%, Sigma-Aldrich), Sulfur (99%, Daejng), Sodium sulfide hydrate (>60%, Sigma-Aldrich), Lead (II) nitrate (99%, Sigma-Aldrich), Cellulose acetate (MW = 29,000, Fluka), Dimethyl Sulfoxide (Sigma-Aldrich), (Cadmium (II) chloride (99.99%, Sigma-Aldrich) and acetone (Sigma-Aldrich) were used as received without any modification.

2.2. Preparation of the TiO_2 electrode

A TiO_2 P90 compact layer was deposited on a pre-cleaned FTO glass plate using the following method. 0.25 g of TiO_2 P90 powder was ground well with 1 ml of 0.1 M HNO_3 for 15 min. This paste was then spin coated on the FTO substrate for 60 s at 3000 rpm and sintered at 450 °C for 45 min. Subsequently a TiO_2 P25 mesoporous layer was deposited on the TiO_2 P90 compact layer by the following method. 0.25 g of TiO_2 P25 powder was ground well with 1 ml of 0.1 M HNO_3, 1 drop of Triton X-100, and 0.05 g of PEG 2000 for 15 min. The P25 paste was deposited on the TiO_2 P90 compact layer by the doctor blading method and sintered at 450 °C for 45 min 14].

2.3. Deposition of CdS quantum dots

Cadmium Sulfide quantum dots were deposited on the TiO_2 film in the photoanode by the successive ionic layer adsorption and reaction (SILAR) method. 0.4 M cadmium chloride ($CdCl_2$) and 0.1 M sodium sulfide (Na_2S) aqueous solutions were prepared for cationic (Cd^{2+}) and anionic (S^{2-}) precursors respectively. For the SILAR method the TiO_2 film was dipped in the cationic precursor for 1 min and thoroughly washed in an ethanol: DI water (1:1) mixture. The same procedure was carried out with the anionic precursor with the same dipping time. 10 SILAR cycles were carried out to fabricate the best CdS QD sensitized TiO_2 photoanode.

2.4. Preparation of PbS quantum dots

PbS quantum dots were deposited on plain glass plate by SILAR method. Six SILAR cycles were performed for preparing the appropriate size of the quantum dots. The materials used were, cationic precursor solution (0.1 M $Pb(NO_3)_2$ in DI water), anionic precursor solution (0.1 M Na_2S in DI water) and each dipping cycle consisting of a 1 min dipping time in Pb^{2+}:Hg^{2+} solution, followed by a 1 min dipping time in S^{2-} solution. Finally, the PbS powder was gently scratched off from the glass plate and used as an additive to the polysulfide electrolyte.

2.5. Preparation of cellulose acetate nanofibers

1 g of cellulose acetate powder, 2 ml of dimethyl sulfoxide (DMSO) and 4 ml of acetone were mixed and the mixture was magnetically stirred for 12 h to get a homogeneous solution. Cellulose acetate nanofibers were deposited on an aluminium sheet in an electrospinning equipment (NaBond Technologies, Hong Kong) with a solution flow rate of 2 ml h^{-1}. During the electrospinning the distance and potential difference between the drum collector and the spinneret were kept at 6.5 cm and 20 kV respectively.

2.6. Preparation of the gel polysulfide electrolyte

Liquid polysulfide electrolyte was prepared by the following method. 2 M sulfur and 2 M Na_2S were dissolved in a mixture of deionized water and methanol in the ratio of 3:7 (v/v). The mixture was continuously stirred until a clear solution was obtained [42,43]. Different amounts of PbS QDs were added to the liquid electrolyte separately. In order to make the gel electrolyte, liquid polysulfide electrolyte was soaked by the cellulose acetate nanofiber membrane [44].

2.7. Optical absorption measurements

In order to study the light absorption by the photoanodes, optical absorption spectra of CdS quantum dot-loaded TiO_2 electrode and the normal TiO_2 electrode were obtained using Shimadzu 2450 UV–VIS spectrophotometer in the wavelength interval from 350 nm to 1100 nm.

2.8. Temperature dependence of the ionic conductivity

Complex impedance measurements of different electrolyte samples were made by using PGSTAT 128 N with FRA 32M Frequency Response Analyzer (Metrohm). For this, the electrolyte was filled between two polished stainless-steel electrodes for each electrolyte and the measurements were taken at temperatures from 30 °C to 70 °C for every 5 °C. Ionic conductivity of the electrolytes was extracted from the complex impedance data.

2.9. DC polarization measurements of the electrolyte

In order to study the ionic and electronic transference numbers of the electrolyte, DC polarization measurements were done by using Metrohm Autolab (PGSTAT 128N) impedance analyzer. Electrolyte was filled between two sulfur electrodes as shown in the Fig. 1 and a fixed DC 0.4 V was applied between the electrodes.

2.10. Cell assembly

A platinum plate was used as the counter electrode. An appropriate amount of the gel polysulfide electrolyte was applied on to the platinum surface. The CdS QD photo anode was placed on the electrolyte so the active sides of the photoanode and the counter electrode were in contact with each other and the solar cell assembly was held together using gently pressed stainless-steel clips.

Fig. 1. (a) Polysulfide electrolyte between two sulfur electrodes and (b) Disc shaped sulfur electrodes.

2.11. Current - output potential difference characterization

In order to compare the photovoltaic performance of the QDSSCs, current density-output potential difference (*J -E*) measurements of solar cells with gel and liquid electrolyte were taken under the illumination of 100 mW cm^{-2} with AM 1.5 spectral filter using a computer controlled multi-meter (Keithley model 2000) coupled with potentiostat/galvanostat unit (HA-301). The active area of the QDSSC was 0.25 cm^2.

2.12. Electrochemical impedance spectra (EIS) measurements

Electrochemical impedance spectra of each QDSSC was obtained by using Metrohm Autolab PGSTAT 128 N coupled to a Metrohm FRA 32M Frequency Response Analyzer under the illumination of 100 mW cm^{-2} (Solar simulator with AM 1.5 spectral filter) in the frequency range from 0.01 Hz to 1 MHz. Carrier transport resistance, recombination resistance and series resistance of the interfaces of the QDSSCs were calculated by fitting the electrochemical impedance spectroscopy (EIS) data with an appropriate equivalent circuit of the QDSSC. Electron lifetimes in the solar cells were also estimated using Bode phase plots.

3. Results and discussion

3.1. Optical absorption spectra

Fig. 2 shows the optical absorption spectra of the TiO_2 electrode and the CdS QDs – sensitized TiO_2 electrode. TiO_2/CdS photoanode shows a broad peak in the visible region from 450 nm to 500 nm which agrees well with previous reports [45].

3.2. Photovoltaic performance

In order to study the effect of PbS QDs in the polysulfide electrolyte, different amounts of PbS QDs were added as different percentages to the polysulfide electrolyte according to the following equation.

$$Percentage\ of\ PbS\ \left(wt/wt\right) = \frac{Mass\ of\ PbS\ QDs}{Mass\ of\ (Na_2S\ +\ S)} \times 100\,\%$$

In order to maintain the clarity the current density-output potential difference (*J-E*) performance of CdS QDSSCs with and without 5% of PbS QDs, under the illumination of 100 mW cm^{-2} with AM 1.5 spectral filter are shown in Fig. 3. The photovoltaic parameters of the solar cells made with liquid polysulfide electrolyte with different amounts of PbS QDs were estimated from the *J-E* curves, and listed in Table 1.

It can be seen that the efficiencies have generally increased with the addition of PbS QDs to the liquid polysulfide electrolyte, and that the maximum efficiency was obtained at 5% (wt/wt) PbS QDs. The main factor determining the efficiency enhancement is the photocurrent density (J_{sc}) as both output potential difference (E_{oc}) and fill factor (*FF*) have remained essentially unchanged for all PbS QD compositions. The J_{sc} value has increased from 8.92 mA cm^{-2} for

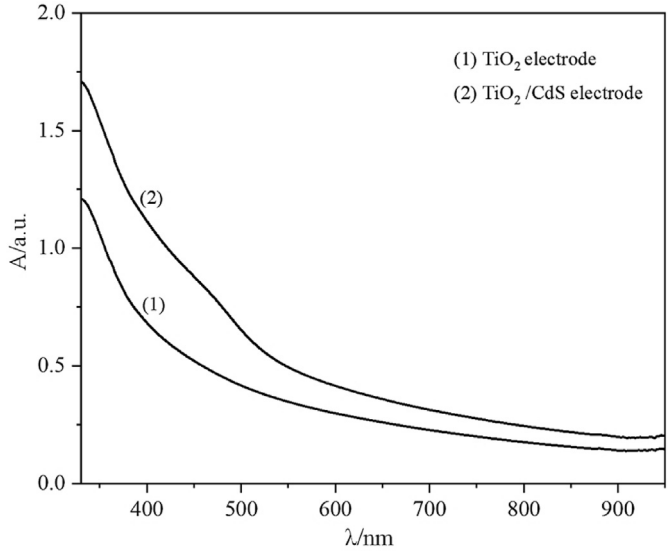

Fig. 2. Optical absorption spectra of the TiO_2 electrode and CdS – sensitized TiO_2 electrode.

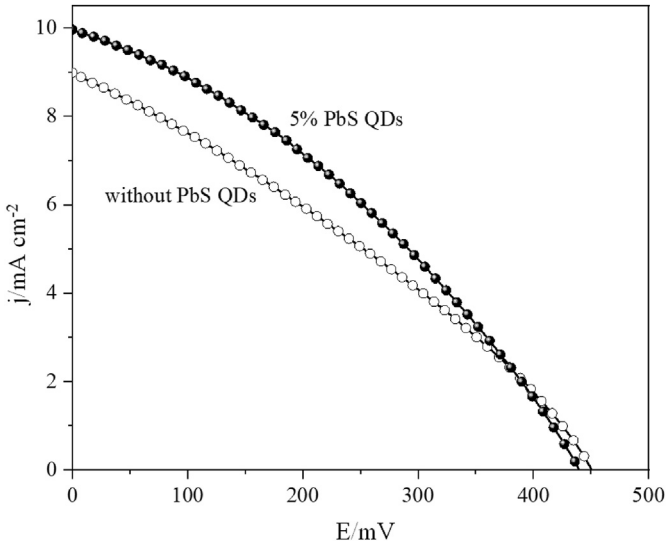

Fig. 3. Current density-output potential difference characterization of the CdS QDSCs with PbS QDs and without PbS QDs in the liquid electrolyte.

Table 1
Photovoltaic parameters of the CdS QDSSCs with different amount of PbS QDs in the liquid polysulfide electrolyte.

Weight % of PbS QDs	J_{SC}/mA cm^{-2}	E_{OC}/mV	*FF* (%)	Efficiency (%)
0%	8.92	445.1	30.01	1.19
2.5%	9.01	455.6	31.65	1.26
5%	9.95	446.1	34.75	1.51
7.5%	9.84	448.3	32.96	1.45
10%	9.64	456.5	31.76	1.40
15%	5.01	455.0	35.89	1.28

the controlled device to a maximum of 9.95 mA cm^{-2} for the PbS QDs added device. This is an 11.5% increase in the photocurrent density.

The modified cells show an overall increase in the efficiencies compared to the controlled device's efficiency of 1.19%, with the maximum at 1.51%. This reflects an efficiency enhancement of 26.9%. The PbS QD added electrolyte appears as a colloidal suspension, as PbS QDs do not undergo ionization and dissolution in the electrolyte medium. Addition of more than 5% of PbS QDs reduces the efficiency of the solar cells.

After optimizing the PbS QD amount in the polysulfide solution electrolyte, cellulose acetate nanofibers were incorporated to the electrolyte to obtain a non-flowing gel electrolyte [44]. Fig. 4 shows a SEM image of the cellulose acetate nanofibre matrix used to form the gel membrane. Fig. 5 shows the photovoltaic parameters of the controlled cell, and the cell with cellulose acetate incorporated nanofibre gel electrolyte. The use of the cellulose acetate nanofiber gel has decreased the efficiency of the control cell as well as the PbS QD added cell as expected due to the decrease in ionic mobility and in the resulting photocurrent. However, out of these two gel electrolyte based cells, the photovoltaic performance of the PbS QD added cell is higher than the control cell.

From Fig. 5 and Table 2 it is clear that the short circuit photocurrent density (J_{sc}) of the gel electrolyte based cell has increased from 3.64 to 5.83 mA cm^{-2} due to incorporation of PbS QDs which is an impressive 60% increase. Correspondingly the cell efficiency has also increased from 0.94% to 1.46% due to PbS QDs in the electrolyte reflecting a remarkable efficiency increase of 55%. Table 2 summarizes the photovoltaic performances parameters of the QDSSCs corresponding to the Fig. 5.

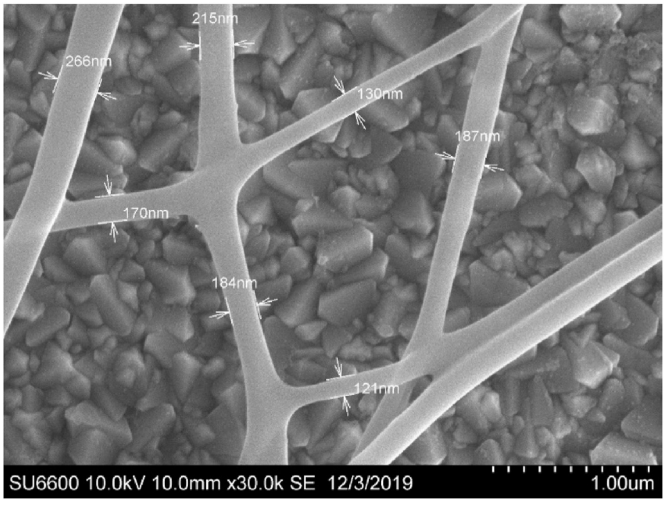

Fig. 4. SEM image of the cellulose acetate nanofibre matrix used to form the gel electrolyte.

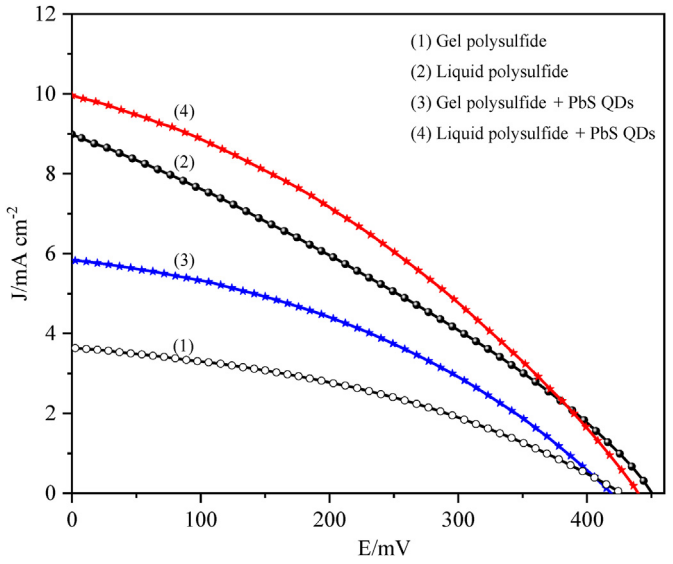

Fig. 5. Current density-output potential difference characterization of the CdS QDSCs with different configurations of polysulfide electrolytes.

Table 2
Photovoltaic parameters of CdS QDSSCs with different electrolyte configurations.

Electrolyte	J_{SC}/mA cm^{-2}	E_{OC}/mV	*FF* (%)	Efficiency (%)
1 - Gel without PbS QDs	3.64	425.1	38.87	0.94
2 - Liquid without PbS QDs	8.92	445.1	30.01	1.19
3 - Gel with PbS QDs	5.83	416.8	38.45	1.46
4 - Liquid with PbS QDs	9.95	446.1	34.75	1.51

3.3. IPCE measurements

To further study the effects of cellulose acetate nanofibers on the CdS QDSSCs, Incident photon to conversion efficiency (IPCE) measurements were taken. Fig. 6 shows the IPCE curves corresponding to solar cells with different gel electrolyte configurations.

As Fig. 6 shows, the addition of PbS QDs to the gel electrolyte has increased the IPCE from 49% to 51% of the CdS QDSSC. The broad IPCE peak from 450 nm to 500 nm conforms with the U–V

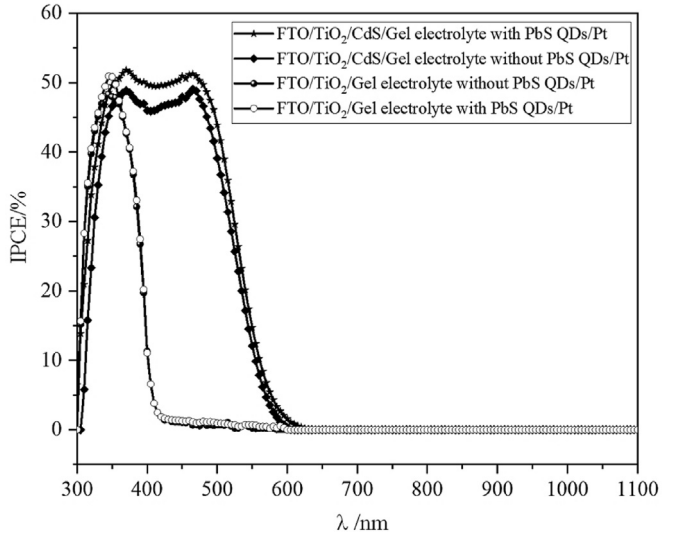

Fig. 6. The IPCE spectra of CdS QDSSCs with different gel electrolyte configurations.

absorption spectra data of the CdS QDs, which shows a similar broad peak from 450 nm to 500 nm (Fig. 2). The absence of the IPCE peak corresponding to the PbS QDs [46,47] confirmed that the efficiency enhancement by the increase in photocurrent is not due to the light absorption by the PbS Q dots.

To further support the absences of an IPCE curve corresponding to PbS QDs, gel based solar cells with and without PbS QDs were assembled without fabricating CdS QDs on the TiO_2 film. The IPCE curves corresponding to these two solar cells were identical, which confirms the absence of an IPCE peak corresponding to PbS QDs. Hence, it can be confirmed that PbS QDs only increases the IPCE of CdS QDSSCs.

3.4. Electrochemical impedance spectroscopy (EIS)

The EIS measurements were taken to investigate the interface resistances and the effect of cellulose acetate nanofiber incorporation. In this study, EIS measurements were carried out under the illumination of 100 mW cm^{-2}. All the devices were fabricated with sulfide electrolyte comprising with 5% PbS QDs. Fig. 7 shows the Nyquist plots corresponding to CdS QDSSCs assembled using either liquid electrolyte with PbS QDs or gel electrolyte with PbS QDs.

In the equivalent circuit diagram in Fig. 7, R_s represents the series resistance of the QDSSC, R_{1CT} and CPE_1 represent resistance and capacitance at the cathode (Pt counter electrode) and electrolyte interface respectively and R_{2CT} & CPE_2 represent the resistance and capacitance at the TiO_2 photoanode and the electrolyte interface respectively. Table 3 shows the resistance values corresponding to each of the interfaces. W is the finite Warburg element which is related to ion diffusion process which are influenced by the behaviour of the TiO_2 photoanode/electrolyte interface and the counter electrode/electrolyte interface. Z_W is the Warburg impedance.

CPE_1 and CPE_2 are the constant phase elements of the counter electrode/electrolyte and photoanode/electrolyte interfaces respectively.

Impedance of the CPE is given by

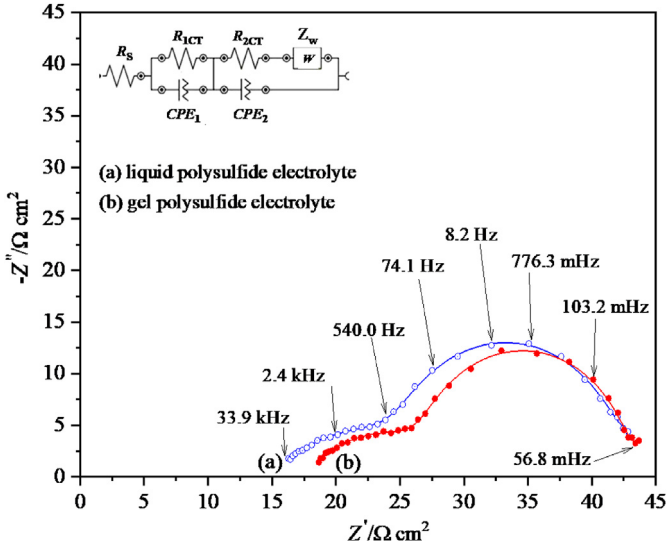

Fig. 7. Nyquist plots of CdS QDSCs with 5% PbS QDs in the liquid and gel electrolytes (line curves denote the calculated spectra and the scatter plots denote the experimental spectra).

$$Z_{CPE} = \frac{1}{Y(j\omega)^n}$$

where Y is the admittance of an ideal capacitor and n is an empirical constant, ranging from 0 to 1.

It can be seen that gelation of the liquid electrolyte has not drastically affected on the interfacial resistance of the devices. Gelation of the liquid electrolyte has decreased the R_{2CT} values from 14.5 Ω cm^2 to 13.9 Ω cm^2 and R_{1CT} values from 11.6 Ω cm^2 to 9.8 Ω cm^2. This reflects the increase in the charge recombination from the photoanode to the electrolyte and counter electrode to the electrolyte, effectively causing an acute reduction of V_{OC} and J_{SC} (Table 2). Similar trends have been reported previously but with different systems [21,33]. Liquid electrolyte shows a smaller Z_W value than the gel electrolyte. Due to the gelation, the diffusion of the ions is hindered. Z_{CPE1} value of liquid electrolyte is lower than the gel electrolyte. Smaller capacitance indicating faster charge transport across the interface is mainly related to collection of a greater number of photo-exited electrons into the conduction band of photoanode due to low recombination [37].

The electron life times were calculated using the Bode phase curves shown in Fig. 8. It can be seen that the incorporation of cellulose acetate nanofiber to the liquid electrolyte has upper shifted the peak frequency from 14.49 Hz to 18.08 Hz (See Table 4).

Electron lifetimes are calculated according to the following equation.

$$Electron\ lifetime = \frac{1}{2\pi f_{max}}$$

where, f_{max} is the frequency corresponding to the peak.

The electron lifetime (τ) is directly proportional to the recombination resistance (R_3), which is consistent with the corresponding values shown in Table 2.

3.5. DC polarization results

The DC polarization curves can be used to understand the effect of PbS QDs addition to the polysulfide electrolyte. Fig. 9 shows the DC polarization curves corresponding to liquid polysulfide electrolytes with varying amounts of PbS QDs. The top six curves were taken using non-blocking, sulfur pellet electrodes in the Pt/S/electrolyte/S/Pt configuration. In order to determine the electronic conductivity, DC polarization curve was also taken using stainless steel (SS) electrodes for the electrolyte without PbS QDs (bottom most curve). It can be seen that the electronic conductivity is negligibly small compared to the ionic conductivity.

Anionic transference number t_{anion} is given by

$$t_{anion} = \frac{I}{I_0}$$

where I is the steady state current and I_o is the initial current at time zero.

From Figs. 9 and 10, it can be concluded that the addition of PbS QDs to the electrolyte has generally increased the sulfide ion (S^{2-}) transference number compared to the electrolyte without PbS QDs. The maximum sulfide ion transference number of 0.73 was exhibited by the electrolyte with 5% PbS QDs. A similar trend can be observed corresponding to J_{SC} values, where 5% PbS QDs exhibits the highest J_{SC} and efficiency values (Table 1). Therefore, the increase of J_{SC} can clearly be attributed to the increase of sulfide ion (S^{2-}/S_n^{2-}) conductivity in the electrolyte.

Table 3
EIS parameters of CdS QDSSCs with 5% PbS QDs in the liquid and gel electrolytes.

Cell	R_S/Ω cm^2	R_{1CT}/Ω cm^2	R_{2CT}/Ω cm^2	Z_{CPE1}/Ω cm^2	Z_{CPE2}/Ω cm^2	Z_W/Ω cm^2
Liquid polysulfide	15.5	11.6	14.5	6.3	5.8	6.3
Gel polysulfide	17.9	9.8	13.9	7.5	6.1	8.1

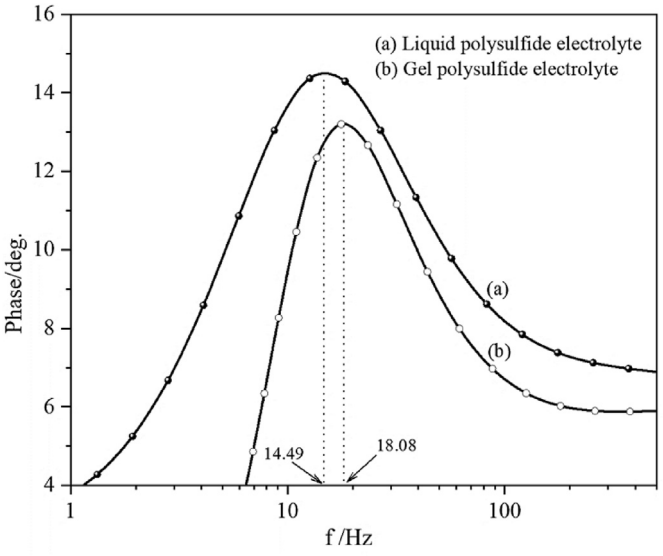

Fig. 8. Bode phase plots of CdS QDSSCs with 5% PbS QDs in the liquid and gel electrolytes.

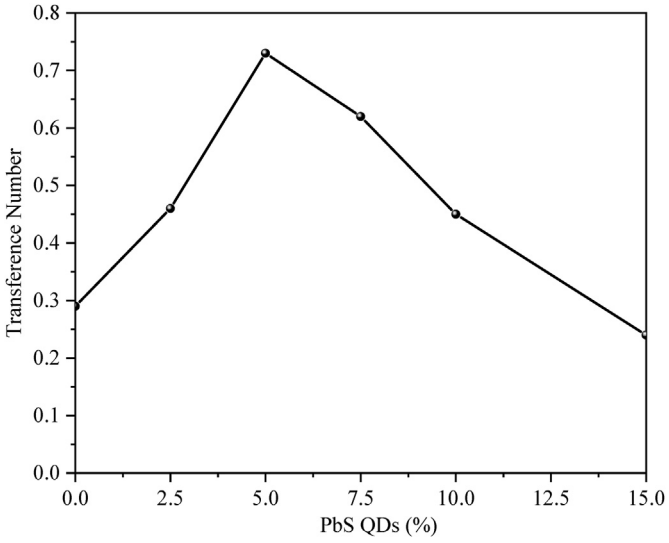

Fig. 10. Variation of anionic transference number with amount of PbS QD added to the polysulfide electrolytes.

Table 4
Comparison of electron lifetime and photovoltaic parameters of CdS QDSSCs.

Electrolyte	f_{max}/Hz	τ/ms	J_{SC}/mA cm^{-2}	Efficiency (%)
Liquid	14.49	10.98	9.95	1.51
Gel	18.08	8.80	5.83	1.46

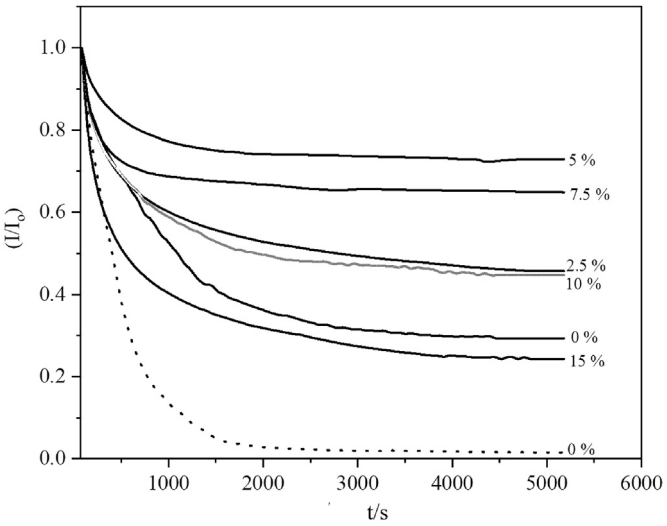

Fig. 9. DC polarization curves of liquid polysulfide electrolytes with different amounts of PbS QDs taken using sulfur pellet electrodes (upper six curves) and using stainless steel electrodes (bottom curve).

3.6. Sulfide ion conductivity

In a polysulfide based Q Dot sensitized solar cell, the bisulphide ion (S^{2-}) conductivity in the electrolyte plays a major role in determining the short circuit photocurrent density and hence the solar cell efficiency. However, to the best of our knowledge, there are no published detailed reports on this subject. Sulfur is generally added to the Na_2S containing electrolyte to obtain a regenerative polysulfide (S^{2-}/S_x^{2-}) redox couple which is vital for the action of these solar cells.

Oxidation reaction occurs at the TiO_2 photoanode-electrolyte interface according to following equations:

$$S^{2-} + 2h^+ \rightarrow S, \quad (1)$$

$$S + S_{x-1}^{2-} \rightarrow S_x^{2-} \ (x = 2\text{–}5) \quad (2)$$

Reduction reaction occurs at the counter electrode, where S_x^{2-} is reverted back to S^{2-}

$$S_x^{2-} + 2e^- \rightarrow S_{x-1}^{2-} + S^{2-} \quad (3)$$

As seen from these redox reactions, the active species at the photoanode are the bisulfide ions S^{2-} and the short circuit photocurrent density, J_{sc} in the solar cell is determined by the transport of bisulfide ions. The ionic conductivity is therefore primarily due to the bisulfide ion conductivity which depends on the mobility and carrier concentration of S^{2-} ions in the electrolyte.

3.7. Temperature dependent conductivity of the electrolyte

The linear variation of ln (σT) vs 1/T shown in Fig. 12 suggests the agreement with the Arrhenius equation, which can be modified to obtain,

$$\sigma T = B\, exp\left(\frac{-E_a}{KT}\right)$$

where E_a is the activation energy, B is the pre exponential factor, and K is the Boltzmann constant.

As seen from Fig. 12, the gradients of the linear graphs are essentially the same for all four electrolyte configurations and independent of the presence of PbS QDs. This implies that the activation energy of 0.12 eV is the same for all four electrolytes. The addition of PbS QDs or the gelation of the liquid polysulfide electrolyte by cellulose acetate nanofibres has not affected the ionic activation process in the electrolyte. This has to be expected as the nanofibre gel electrolyte is essentially the liquid electrolyte "trapped" within the cages of the nanofibre matrix. Another very important observation can be made from the points of intersection of the extrapolated linear Arrhenius plots in Fig. 12 with the y-axis. These points of intersection correspond to the pre-exponential factors which are proportional to the carrier concentration in the respective electrolytes. Based on this analysis, it can be clearly seen that the addition of PbS QDs to the liquid polysulfide electrolyte as well as to the nanofibre gel polysulfide electrolyte have substantially increased the concentration of free S^{2-} ions in the electrolyte.

Proposing a mechanism to explain the observed ionic conductivity increase due to the incorporation of 5 wt% of PbS Q dots in the polysulfide electrolyte is not straight forward. To the best of our knowledge there are no published reports on similar systems with possible explanations. Singh et al. have reported an efficiency increase in a dye sensitized solar cell based on PEO solid polymer electrolyte due to the addition of ZnS capped CdSe QD doped into the electrolyte medium but no explanation is given on a mechanism for the observed efficiency increase [50]. Duan et al. [39] has reported that in their solid-state dye-sensitized solar cells based on iodide/tri-iodide(I^-/I_3^-)-incorporated poly(ethylene oxide)/polyaniline(PEO/PANI) solid-state electrolytes, PANI enhances catalytic and hole-transporting characteristics while participating in dye regeneration as well. We, however, proposing a quite different mechanism here to explain our experimental observations.

In our work, the addition of PbS QDs to the polysulfide electrolyte has substantially increased the anionic transference number, as shown by the DC polarization curves in Fig. 8 and also by the increased ionic conductivity as depicted in Figs. 9 and 11. Since the optical absorption peak in the in the IPCE curve (Fig. 6) corresponding to PbS QDs is absent, it can be conclusively stated that PbS QDs in the electrolyte do not generate any extra ionic species by electron-hole pair creation under illumination.

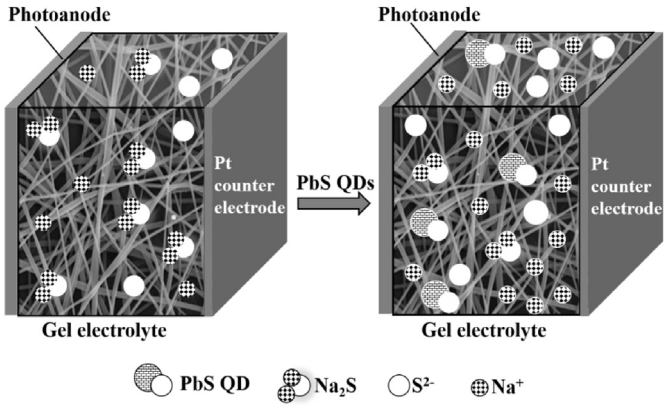

Fig. 11. Schematic diagram of the nanofibre gel electrolyte based solar cells with and without PbS Q-dots in the electrolyte.

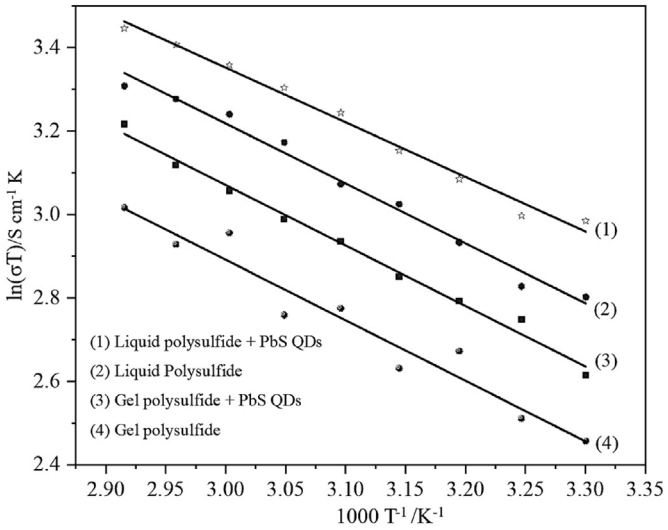

Fig. 12. ln(σT) vs 1000/T for different electrolyte configurations used in this work.

PbS is not an ionic compound and does not dissolve in the electrolyte medium and therefore does not provide additional sulfide ions through direct ionic dissociation of this compound. Visibly also, the PbS Q dots added to the polysulfife liquid electrolyte remain undissolved and appear as a suspension. Further, there are no evidence to show that PbS Q dots directly facilitate ionic dissociation in the polysulfide electrolyte. Therefore, one or both of the following two mechanisms could be proposed to explain the observed increase in the ionic conductivity and the anionic transference number and hence the photocurrent density due to the addition of 5 wt% of PbS Q dots to the liquid electrolyte.

(a) It has been reported that following the synthesis of colloidal PbS Q dots, the native hydroxyl groups (OH−) could get attached to the surface of PbS QDs on the (111) facets and improve their stability [48]. The presence of hydroxide species at the PbS QD surface has been qualitatively demonstrated and charge neutrality may result also from reduced Pb atoms (i.e., in the 1+ or, the more likely, 0 oxidation state). There is a possibility for these OH− surface hydroxyl groups to form coordination bonds with Na^+ ions from the undissociated Na_2S species in the polysulfide electrolyte leaving more free bisulfide (S^{2-}) ions thereby indirectly promoting ionic dissociation and increasing the number of free sulfide ions and hence the conductivity. This is consistent also with conclusions drawn from Fig. 12. ln(σT) vs 1000/T variation.

(b) Metal ions can be adsorbed by QDs either via electrostatic attraction or ligand coordination. Since the metal ions are typically electron-deficient, electron transfer from the conduction band of the QDs to metal ions can occur. In the present example, there is a possibility for Na+ ions in undissociated Na2S in the electrolyte to get adsorbed by the PbS QD leaving free sulfide ions (S2-) available for ionic transport [49].

Addition of PbS Q dots beyond the optimum concentration of 5 wt% will have a negative effect on conductivity quite likely due to the blocking affect due to the presence of excessive PbS QDs and resulting spatial hindrance for the bisulfide (S^{2-}) ion transport. At higher PbS concentrations, there exists also the possibility of forming more complex ions and ionic aggregates with S^{2-} ions thereby reducing the number of S^{2-} ions available for ionic

transport while at the same time reducing the effective ionic mobility.

4. Conclusion

In summary, the addition of PbS QDs to the polysulfide electrolyte increases the efficiency of CdS QDSSC from 1.46% to 1,74% for liquid electrolyte based cells and from 1.16% to 1.48% for the gel electrolyte based cells. The observed efficiency increase has been attributed to the dramatic increase in the short circuit photocurrent density J_{SC} by more than 25% evidently due to the increased bisulfide ion conductivity. It is very likely that the PbS QDs facilitate indirect ionic dissociation of the polysulfide electrolyte thereby increasing the concentration of mobile bisulfide (S^{2-}) ions. The incorporation of cellulose acetate nanofiber to the PbS QD added liquid electrolyte results in a more stable, non-flowing gel state CdS QDSSC.

Declaration of competing interest

The authors declare that they have no known competing financial interests or personal relationships that could have appeared to influence the work reported in this paper.

CRediT authorship contribution statement

M.A.K.L. Dissanayake: Conceptualization, Methodology, Supervision, Writing - review & editing. **T. Liyanage:** Data curation, Writing - original draft. **T. Jaseetharan:** Supervision. **G.K.R. Senadeera:** Supervision, Writing - review & editing. **B.S. Dassanayake:** Conceptualization.

Acknowledgment

The Authors gratefully acknowledge the financial support provided by the National Science Foundation of Sri Lanka under grant number NSF/SCH/2018/04.

Appendix A. Supplementary data

Supplementary data to this article can be found online at https://doi.org/10.1016/j.electacta.2020.136311.

References

[1] K.W.J. Barnham, M. Mazzer, B. Clive, Resolving the energy crisis: nuclear or photovoltaics, Nat. Mater. 5 (2006) 161–164.
[2] H. Tada, M. Fujishima, H. Kobayashi, Photo deposition of metal sulfide quantum dots on titanium(iv) dioxide and the applications to solar energy conversion, Chem. Soc. Rev. 40 (2011) 4232–4243.
[3] M.C. Beard, J.M. Luther, A.J. Nozik, The promise and challenge of nanostructured solar cells, Nat. Nanotechnol. 9 (2014) 951–954.
[4] A.J. Nozik, Quantum dot solar cells, Phys. E Low-dimens. Syst. Nanostruct. 14 (2002) 115–120.
[5] C.-H.M. Chuang, P.R. Brown, V.B. Moungi, G. Bawendi, Improved performance and stability in quantum dot solar cells through band alignment engineering, Nat. Mater. 13 (2014) 796–801.
[6] I. Mora-Seró, J. Bisquert, Breakthroughs in the development of semiconductor-sensitized solar cells, J. Phys. Chem. Lett. 1 (20) (2010) 3046–3052.
[7] P.V. Kamat, Quantum dot solar cells. The next big thing in photovoltaics, J. Phys. Chem. Lett. 4 (6) (2013) 908–918.
[8] S. Rühle, M. Shalom, A. Zaban, Quantum-dot-sensitized solar cells, ChemPhysChem 11 (2010) 2290–2304.
[9] I. Barceló, T. Lana-Villarreal, R. Gómez, Efficient sensitization of ZnO nanoporous films with CdSe QDs grown by successive ionic layer adsorption and reaction (SILAR), J. Photochem. Photobiol. A Chem. 220 (2011) 47–53.
[10] A. Tubtimtae, K.-L. Wu, H.-Y. Tung, M.-W. Lee, G.J. Wang, Ag_2S quantum dot-sensitized solar cells, Electrochem. Commun. 12 (2010) 1158–1160.
[11] Y. Lee, Y. Lo, Highly efficient quantum-dot-sensitized solar cell based on co-sensitization of CdS/CdSe, Adv. Funct. Mater. 19 (2009) 604–609.
[12] P. Yu, K. Zhu, A.G. Norman, S. Ferrere, A.J. Frank, A.J. Nozik, Nanocrystalline TiO_2 solar cells sensitized with InAs quantum dots, J. Phys. Chem. B 110 (50) (2006) 25451–25454.
[13] W. Wang, W. Feng, J. Du, W. Xue, L. Zhang, L. Zhao, Y. Li, X. Zhong, Cosensitized quantum dot solar cells with conversion efficiency over 12%, Adv. Mater. 30 (2018), 1705746.
[14] J. Du, Z. Du, J.-S. Hu, Z. Pan, Q. Shen, J. Sun, D. Long, H. Dong, L. Sun, X. Zhong, L.-J. Wan, Zn–Cu–In–Se quantum dot solar cells with a certified power conversion efficiency of 11.6%, J. Am. Chem. Soc. 138 (12) (2016) 4201–4209.
[15] L.-L. Tan, J.-F. Huang, Y. Shen, L.-M. Xiao, J.-M. Liu, D.-B. Kuang, C.-Y. Su, Highly efficient and stable organic sensitizers with duplex starburst triphenylamine and carbazole donors for liquid and quasi-solid-state dye-sensitized solar cells, J. Mater. Chem. A 2 (2014) 8988–8994.
[16] M. Mingsukang, M. Buraidah, M.A. Careem, Development of gel polymer electrolytes for application in quantum dot-sensitized solar cells, Ionics 23 (2017) 347.
[17] W. Feng, Y. Li, J. Du, W. Wanga, X. Zhong, Highly efficient and stable quasi-solid-state quantum dot-sensitized solar cells based on a superabsorbent polyelectrolyte, J. Mater. Chem. A 4 (2016) 1461–1468.
[18] H. Kim, I. Hwang, K. Yong, Highly durable and efficient quantum dot-sensitized solar cells based on oligomer gel electrolytes, ACS Appl. Mater. Interfaces 6 (14) (2014) 11245–11253.
[19] Z. Du, H. Zhang, H. Bao, X. Zhong, Optimization of TiO_2 photoanode films for highly efficient quantum dot-sensitized solar cells, J. Mater. Chem. A 2 (2014) 13033–13040.
[20] J.M.K.W. Kumari, G.K.R. Senadeera, M.A.K.L. Dissanayake, Dependence of photovoltaic parameters on the size of cations adsorbed by TiO_2 photoanode in dye-sensitized solar cells, Ionics 23 (2017) 2895–2900.
[21] M.A.K.L. Dissanayake, T. Jaseetharan, G.K.R. Senadeera, C.A. Thotawattage, A novel, PbS:Hg quantum dot-sensitized, highly efficient solar cell structure with triple layered TiO_2 photoanode, Electrochim. Acta 269 (2018) 172–179.
[22] K. Pralay, P.V. Kamat, Mn-doped quantum dot sensitized solar cells: a strategy to boost efficiency over 5%, J. Am. Chem. Soc. 134 (5) (2012) 2508–2511.
[23] Y. Yang, Q. Zhang, T. Wang, L. Zhu, X. Huang, Y. Zhang, X. Hu, D. Li, Y. Luo, Q. Meng, Novel tandem structure employing mesh-structured Cu2S counter electrode for enhanced performance of quantum dot-sensitized solar cells, Electrochim. Acta 88 (2013) 44–50.
[24] Z. Tachan, M. Shalom, I. Hod, S. Rühle, S. Tirosh, A. Zaban, PbS as a highly catalytic counter electrode for polysulfide-based quantum dot solar cells, J. Phys. Chem. C 115 (13) (2011) 6162–6166.
[25] H. Chen, L. Zhu, H. Liu, W. Li, ITO porous film-supported metal sulfide counter electrodes for high-performance quantum-dot-sensitized solar cells, J. Phys. Chem. C 117 (8) (2013) 3739–3746.
[26] S. Jiao, J. Du, Z. Du, D. Long, W. Jiang, Z. Pan, Y. Li, X. Zhong, Nitrogen-doped mesoporous carbons as counter electrodes in quantum dot sensitized solar cells with a conversion efficiency exceeding 12%, J. Phys. Chem. Lett. 8 (3) (2017) 559–564.
[27] T. Yasuhiro, A. Hitomi, O. Yasuhide, T. Tsukasa, K. Susumu, CdS quantum dots sensitized TiO_2 sandwich type photoelectrochemical solar cells, Chem. Lett. 36 (1) (2007) 88–89.
[28] G. Niu, L. Wang, R. Gao, B. Ma, H. Dong, Y. Qiu, Inorganic iodide ligands in ex situ PbS quantum dot sensitized solar cells with I^-/I_3^- electrolytes, J. Mater. Chem. 22 (2012) 16914–16919.
[29] V. Jovanovski, V. González-Pedro, S. Giménez, E. Azaceta, G. Cabañero, H. Grande, R. Tena-Zaera, I. Mora-Seró, J. Bisquert, A sulfide/polysulfide-based ionic liquid electrolyte for quantum dot-sensitized solar cells, J. Am. Chem. Soc. 133 (50) (2011) 20156–20159.
[30] S.D. Sung, I. Lim, P. Kang, C. Lee, W.I. Lee, Design and development of highly efficient PbS quantum dot-sensitized solar cells working in an aqueous polysulfide electrolyte, Chem. Commun. 49 (2013) 6054–6056.
[31] J. Du, X. Meng, K. Zhao, Y. Li, X. Zhong, Performance enhancement of quantum dot sensitized solar cells by adding electrolyte additives, J. Mater. Chem. A 3 (2015) 17091–17097.
[32] J. Yu, W. Wang, Z. Pan, J. Du, Z. Ren, W. Xue, X. Zhong, Quantum dot sensitized solar cells with efficiency over 12% based on tetraethyl orthosilicate additive in polysulfide electrolyte, J. Mater. Chem. A 5 (2017) 14124–14133.
[33] Y. Sun, G. Jiang, M. Zhou, Z. Pan, X. Zhong, Origin of the effects of PEG additives in electrolytes on the performance of quantum dot sensitized solar cells, RSC Adv. 8 (2018) 29958–29966.
[34] L. Li, X. Yang, J. Gao, H. Tian, J. Zhao, A. Hagfeldt, L. Sun, Highly efficient CdS quantum dot-sensitized solar cells based on a modified polysulfide electrolyte, J. Am. Chem. Soc. 133 (22) (2011) 8458–8460.
[35] H. Song, H. Rao, X. Zhong, Recent advances in electrolytes for quantum dot-sensitized solar cells, J. Mater. Chem. A 6 (2018) 4895–4911.
[36] S.B. Patel, J.V. Gohel, Quasi solid-state quantum dot–sensitized solar cells with polysulfide gel polymer electrolyte for superior stability, J. Solid State Electrochem. 23 (2019) 2657–2666.
[37] H.-J. Kim, D.-J. Kim, S.S. Rao, A.D. Savariraj, K. Soo-Kyoung, M.-K. Son, C.V.V.M. Gopi, K. Prabakar, Highly efficient solution processed nanorice structured NiS counter counterelectrode for quantum dot sensitized solar cells, Electrochim. Acta 127 (2014) 427–432.
[38] Z. Huo, L. Tao, S. Wang, J. Wei, J. Zhu, W. Dong, F. Liu, S. Chen, B. Zhang, S. Dai, A novel polysulfide hydrogel electrolyte based on low molecular mass organogelator for quasi-solid-state quantum dot-sensitized solar cells, J. Power Sources 284 (2015) 582–587.
[39] J. Duan, Q. Tang, R. Li, B. He, L. Yu, P. Yang, Multifunctional graphene

incorporated polyacrylamide conducting gel electrolytes for efficient quasi-solid-state quantum dot-sensitized solar cells, J. Power Sources 284 (2015) 369–376.
[40] E. Raphael, D.H. Jara, M.A. Schiavon, Optimizing photovoltaic performance in $CuInS_2$ and CdS quantum dot-sensitized solar cells by using an agar-based gel polymer electrolyte, RSC Adv. 7 (2017) 6492–6500.
[41] O. Regan, M. Gratzel, A low-cost, high-efficiency solar cell based on dye-sensitized colloidal TiO_2 films, Nature 353 (1991) 737–740.
[42] H.K. Jun, M.A. Careem, A.K. Arof, A suitable polysulfide electrolyte for CdSe quantum dot-sensitized solar cells, Int. J. Photoenergy 10 (2013), 942139.
[43] Y.-L. Lee, C.-H. Chang, Efficient polysulfide electrolyte for CdS quantum dot-sensitized solar cells, J. Power Sources 185 (2008) 584–588.
[44] A.M.J.S. Weerasinghe, M.A.K.L. Dissanayake, G.K.R. Senadeera, V.A. Senaviratne, C.A. Thotawatthage, J.M.K.W. Kumari, Application of electrospun cellulose acetate nanofibre membrane based quasi-solid-state electrolyte for dye sensitized solar cells, Ceylon J. Sci. 46 (2) (2017) 93–98.
[45] B.R. Sankapal, R.S. Mane, C.D. Lokhande, Deposition of CdS thin films by the successive ionic layer adsorption and reaction (SILAR) method, Mater. Res. Bull. 35 (2) (2000) 177–184.
[46] H. Lee, H.C. Leventis, S. Moon, P. Chen, S. Ito, S.A. Haque, T. Torres, F. Nüesch, T. Geiger, S.M. Zakeeruddin, M. Grätzel, M.K. Nazeeruddin, PbS and CdS quantum dot-sensitized solid-state solar cells: “Old concepts, new results”, Adv. Funct. Mater. 19 (2009) 2735–2742.
[47] L. Lai, L. Protesescu, M.V. Kovalenko, M.A. Loi, Sensitized solar cells with colloidal PbS–CdS core–shell quantum dots, J. Phys. Chem. Chem. Phys. 16 (2014) 736–742.
[48] D. Zherebetskyy, M. Scheele, Y. Zhang, N. Bronstein, C. Thompson, D. Britt, M. Salmeron, P. Alivisatos, L.-W. Wang, Hydroxylation of the surface of PbS nanocrystals passivated with oleic acid, Science 344 (2014) 1380–1384.
[49] P. Wu, T. Zhao, S. Wang, X. Hou, Semiconductor quantum dots-based metal ion probes, Nanoscale 6 (2014) 43–64.
[50] P.K. Singh, K.W. Kim, H.-W. Rhee, Quantum dot doped solid polymer electrolyte for device application, Electrochem. Commun. 11 (2009) 1247–1250.